Nonlinear Intermodulation Coupling in Ferrite Circulator Junctions

Hoton How, Carmine Vittoria, *Fellow, IEEE,* and Ronald Schmidt, *Fellow, IEEE*

***Abstract*— We have solved the nonlinear intermodulation coupling problem of a planar ferrite junction containing $3N$ ports. The coupling is represented as driving currents within the junction, and the induced fields can be solved by using the radiation and the boundary-value Green's functions. Maximum coupling of intermodulations occur if the excitation frequencies at the ports are close to the circulation frequency of the circulator. Also, we find that the static demagnetizing field can effectively increase the intermodulation output power.**

***Index Terms*— Ferrite device, gyromagnetic property, intermodulation, junction circulator, nonlinear interaction.**

I. Introduction

IN HIGH-POWER systems a high-power circulator (isolator) is indispensable to protecting the high-power source from instability and deterioration due to reflected power from the load. Among many important applications, power circulators are generally required for cellular phone communication systems where the maximum emission power can be as high as 30 W. Under high-power excitations, the motion of the magnetization vector can no longer be described by a linearized set of equations. Considering next-order (cubic) terms in the equation of motion echo signals in the time domain [1], [2] and intermodulation coupling in the frequency domain [3] must be included in a nonlinear theory. In the past, How *et al.* have formulated [1], [2] the mechanism for echoing in a ferrite junction. Prediction from our mechanism was in full agreement with experimental data [1], [2]. However, the intermodulation coupling is less understood, although an initial primitive treatment can be found in [3].

Intermodulation signals grow rapidly with power. For input power below 1 W, the level of the induced intermodulation is in general -100 dB below the input signals [3]. However, when signal levels are increased to 30 W, the intermodulation noises acquire a power of -70 dB below the input signals. They are identified as clicking noises in a telephone line. The reduction of nonlinear intermodulation noises in ferrite junctions is therefore of crucial importance for cellular phone communications, not only to improve the quality of the telephone signals, but also to allow fewer radio stations to be distributed in the transmission network.

Manuscript received February 2, 1996; revised October 18, 1996.

H. How was with Massachusetts Technological Laboratory, Inc., Belmont, MA 02178 USA. He is now with ElectroMagnetic Applications, Inc., Boston, MA 02109 USA.

C. Vittoria is with the Electrical and Computer Engineering Department, Northeastern University, Boston, MA 02115 USA.

R. Schmidt is with the Microelectronics Products Division, Radar Products Operations, M/A-COM., Inc., Burlington, MA 01803 USA.

Publisher Item Identifier S 0018-9480(97)00829-6.

Previous theoretical formulation [3] on intermodulation was derived ad hoc from the equation of motion of the magnetization vector which gives rise to at best an order of estimate about this coupling effect. In [3] the equation of motion was iterated to high orders without restricting the magnetization vector to be of constant magnitude. The resultant nonlinear magnetic equation was then solved by assuming the induced intermodulation magnetic field to be identically zero. This assumption negates the coupling between the magnetization vector and other RF-electromagnetic fields via Maxwell equations. In fact, by setting the intermodulation magnetic field to zero, it is not feasible to generate intermodulation power. Also, the theory of Wu *et al*. excluded a treatment on the demagnetizing field of the ferrite junction. It was pointed out by [4] that the static demagnetization is closely related to the microwave instability occurring at the subsidiary absorption for ferrimagnetic resonance measurements. Also, How *et al*. [1], [2] have shown that the static demagnetization can substantially reduce the measured ferrimagnetic echo gain to zero. In this paper, we will show that the demagnetizing field of the ferrite junction can significantly enhance the intermodulation coupling in a ferrite circulator junction.

In this paper we first expand the equation of motion of the magnetization vector to the third power of the excited RF-fields. Cubic intermodulation is identified as inhomogeneous terms in the magnetic constituent equation relating the RF-magnetization field to the RF-magnetic displacement fields. Maxwell equations are then cast in the form of Helmholtz equations with an effective current source appearing on the right-hand side (RHS). Therefore, the intermodulation coupling is solved as a two-dimensional (2D) radiation problem and the induced fields are obtained through the use of Green's functions. Two kinds of Green's functions are needed. The first kind of Green's function gives outgoing waves generated from a δ-function distributed point source in the junction. The second kind of Green's function is derived from a source-free junction; it is required to cancel the tangential RF-fields at the ferrite junction boundary to satisfy the boundary conditions there. The final functional form of the intermodulation field is expressed as a double integral over the junction area which can then be evaluated numerically by using finite-difference methods.

Our calculations have been applied to the three-port power circulator previously reported in [3]. We have shown that intermodulation coupling results in maximum power output if the primary signals are excited near the center transmission frequency of the circulator. The calculated intermodulation

levels compare very well with measurements reported in [3]. The effect of static demagnetization has also been calculated. It will be shown that by decreasing the axial demagnetizing factor of the ferrite junction from one to one-third the output intermodulation power can be correspondingly reduced by about 5–6 dB. Finally, different phases of the excitation signals have been incorporated in the calculations, revealing the interference nature of the intermodulation coupling. This paper is organized as follows. In Section II the theoretical formulation of the equation of motion is developed. When coupled with Maxwell equations, the modulation field is then described by Helmholtz equations which are solved by using Green's functions. Section III includes results of the calculations considering a power circulator design reported in [3]. Conclusions follow in Section IV.

II. Formulation

Within a ferrimagnetic substance the magnetization vector $\underline{\boldsymbol{M}}$ satisfies the following equation of motion:

$$\frac{\partial \underline{\boldsymbol{M}}}{\partial t} = -\gamma \underline{\boldsymbol{H}}_{\text{eff}} \times \underline{\boldsymbol{M}} \tag{1}$$

where the effective field can be derived from a given energy distribution $w(\underline{\boldsymbol{M}}, \partial \underline{\boldsymbol{M}}/\partial x_i)$ as [5]

$$(\underline{\boldsymbol{H}}_{\text{eff}})_i = -\frac{\partial w}{\partial M_i} + \sum_{j=1}^{3} \frac{\partial}{\partial x_j} \frac{\partial w}{\partial (\partial M_i/\partial x_j)}. \tag{2}$$

Here w can depend not only on magnetization vector $\underline{\boldsymbol{M}}$, but also on the magnetic strains $\partial \underline{\boldsymbol{M}}/\partial x_j$. The most general $\underline{\boldsymbol{H}}_{\text{eff}}$ includes the following components:

$$\underline{\boldsymbol{H}}_{\text{eff}} = H_o \underline{\boldsymbol{e}}_z + \underline{\boldsymbol{h}} + \underline{\boldsymbol{h}}_A + \underline{\boldsymbol{h}}_E + \underline{\boldsymbol{h}}_\gamma + \underline{\boldsymbol{h}}_d + \underline{\boldsymbol{h}}_s \tag{3}$$

where

- H_o external field;
- $\underline{\boldsymbol{h}}$ RF field;
- $\underline{\boldsymbol{h}}_d$ dipolar field;
- $\underline{\boldsymbol{h}}_s$ magnetoelastic field;
- $\underline{\boldsymbol{h}}_A = (2K/M_s^2)\underline{\boldsymbol{M}} \cdot \underline{\boldsymbol{e}}_z =$ anisotropy field;
- $\underline{\boldsymbol{h}}_E = (2A/M_s^2)\nabla^2 \underline{\boldsymbol{M}} =$ exchange field;
- $\underline{\boldsymbol{h}}_\lambda = (-\lambda/\gamma M_s)\partial \underline{\boldsymbol{M}}/\partial t =$Gilbert damping field;

and K, A, γ, λ, M_s are, respectively, (uniaxial) anisotropy constant, exchange stiffness, Gilbert damping constant, gyromagnetic ratio ($= 1.76 \times 10^7$ rad $(\sec \cdot Oe)^{-1}$), and saturation magnetization. In (3) $\underline{\boldsymbol{e}}_z$ denotes the unit vector along z-direction, which is not to be confused with a latter symbol of e_z denoting the z-component of the RF-electric field. Under magnetostatic approximation the dipolar or demagnetizing field $\underline{\boldsymbol{h}}_d$ satisfies the following equations:

$$\nabla \cdot \boldsymbol{h}_d = -4\pi \nabla \cdot \underline{\boldsymbol{M}}$$
$$\nabla \times \underline{\boldsymbol{h}}_d = 0.$$

The evaluation of demagnetizing fields for an arbitrary excitation is a fairly complicated problem. It was shown in [1] and [2] that the dipolar field is of crucial importance in correlating nonlocal excitations to create echo signals in a single-crystal yttrium iron garnet (YIG) sample. However, if we assume the lateral dimension of the ferrite is much larger than its thickness, the dipolar field becomes

$$\underline{\boldsymbol{h}}_d = -4\pi N_z \underline{\boldsymbol{M}} \cdot \underline{\boldsymbol{e}}_z \underline{\boldsymbol{e}}_z. \tag{4}$$

This is the situation that is normally assumed for a ferrite circulator junction [6]–[8]. In (4) N_z denotes the (axial) demagnetizing factor. The damping field can be effectively accounted for if one replaces the external field H_o by $H_o - (i\lambda/\gamma)\omega$, or, equivalently [8]

$$H_o \to H_o - \frac{i\Delta H}{2} \frac{f}{f_r} \tag{5}$$

where ΔH is the ferromagnetic resonance (FMR) linewidth measured at frequency f_r. The magnetoelastic field can be derived from the following electroelastic energy density using [5, eq. (2)]:

$$w_s = b_1(\alpha_x^2 \epsilon_{xx} + \alpha_y^2 \epsilon_{yy} + \alpha_z^2 \epsilon_{zz}^2) + 2b_2(\alpha_x \alpha_y \epsilon_{xy} + \alpha_y \alpha_z \epsilon_{yz} + \alpha_z \alpha_x \epsilon_{zx}) \tag{6}$$

where α_i's are the direction cosines of the magnetization vector $\underline{\boldsymbol{M}}$,$\epsilon_{ij}$'s are the strain fields, and b_1 and b_2 are magnetoelastic coupling constants. For the current calculations on nonlinear intermodulation we omit the influence from exchange, anisotropy, and magnetoelastic interactions. However, their roles in junction circulator performance will be discussed in a future paper.

For a large excursion of the magnetization vector we write

$$m_z = M_s - M_z \approx \frac{\underline{\boldsymbol{m}} \cdot \underline{\boldsymbol{m}}}{2M_s} \tag{7}$$

upon which (1) becomes

$$\frac{-1}{\gamma} \frac{d\underline{m}}{dt} = \underline{e}_z \times [H_{\text{in}} \underline{\boldsymbol{m}} - M_s \underline{\boldsymbol{h}} + (h_z + 4\pi N_z m_z)\underline{\boldsymbol{m}} + m_z \underline{\boldsymbol{h}}]. \tag{8}$$

In (8) $\underline{\boldsymbol{m}}$ and $\underline{\boldsymbol{h}}$ denote transverse components of the RF-magnetization and magnetic fields, and the internal field H_{in} is given as

$$\underline{\boldsymbol{H}}_{\text{in}} = (H_o - 4\pi N_z M_s)\underline{\boldsymbol{e}}_z. \tag{9}$$

The z-component of (1) can be shown to be equivalent to the transverse components (8). Note that in (7) we have imposed the constant magnitude condition on the magnetization vector

$$|\underline{\boldsymbol{M}}| = M_s \tag{10}$$

which gives rise to cubic interaction in (8) represented directly by the following two terms:

$$\underline{\boldsymbol{m}} \cdot \underline{\boldsymbol{m}}\, \underline{\boldsymbol{m}} \quad \text{and} \quad \underline{\boldsymbol{m}} \cdot \underline{\boldsymbol{m}}\, \underline{\boldsymbol{h}}. \tag{11}$$

This is in contrast to the equation of motion assumed by Wu *et al.* who derived intermodulation coupling from an iteration scheme, involving second-order excitation in m_z and then third-order excitation in m_ϕ [3]. The magnitude of the magnetization vector is not conserved in the theory of [3], as required by (10). The other difference of our model with respect to [3] is that we have included demagnetizing fields in our formulation. It was pointed out in [4] that the

static demagnetization is closely related to the spin-wave instability occurring in the subsidiary absorption at microwave resonance measurements. For ferrimagnetic echo experiments it was generally known that magnetic demagnetization can significantly reduce the induced echo-gain amplification in the generated echo signals [1], [2]. We will show later in this paper that this same effect can produce higher intermodulation levels and hence its magnitude should be minimized if a noise-free circulator design is desired.

In the following we will discard the term proportional to h_z in (8) since, as it will be discussed below, h_z does not couple to the other major fields, $\underline{\boldsymbol{m}}$, $\underline{\boldsymbol{h}}$, and e_z, through Maxwell equations, and it does not contribute to any net power flow at the intermodulation frequency at the circulator junction ports. We must emphasize here that all of the above derivations are valid only for real (physical) quantities. The commonly used phasor representation of complex fields is meaningless under nonlinear consideration. Nevertheless, (8) can be converted into an effective complex form at the single intermodulation frequency. That is, let the ferrite junction be excited by two monochromatic signals of angular frequency ω_1 and ω_2. Intermodulation coupling through (11) contains the following term:

$$\begin{aligned}&[m_{1\rho}\cos(\omega_1 t+\theta_1)][m_{2\rho}\cos(\omega_2 t+\theta_2)][m_{1\rho}\cos(\omega_1 t+\theta_1)]\\&\quad=(m_{1\rho}^2 m_{2\rho}/8)\cos[(2\omega_1-\omega_2)t+2\theta_2-\theta_1]\\&\qquad+(\text{terms at other frequencies})\end{aligned}$$

and θ_1 and θ_2 denote arbitrary phases. Other terms in (11) can be decomposed in a similar fashion. Therefore, as long as we are considering terms relating to intermodulation excitation at angular frequency $\omega_3(=2\omega_1-\omega_2)$ in (8), complex phasor notations can be resumed provided that the longitudinal RF-magnetization m_z, in (7) is now replaced by

$$m_z=\frac{\underline{\boldsymbol{m}}_1\cdot\underline{\boldsymbol{m}}_2^*}{16M_s}. \tag{12}$$

As such, the equation of motion (8) becomes

$$\frac{-1}{\gamma}\frac{d\underline{m}_3}{dt}=\underline{e}_z\times[H_{\text{in}}\underline{\boldsymbol{m}}_3-M_s(\underline{\boldsymbol{h}}_3-\underline{\alpha})] \tag{13}$$

where the inhomogeneous term $\underline{\alpha}$ is given as

$$\underline{\alpha}=\frac{\underline{\boldsymbol{m}}_1\cdot\underline{\boldsymbol{m}}_2^*}{16M_s^2}(4\pi N_z\underline{\boldsymbol{m}}_1+\underline{\boldsymbol{h}}_1). \tag{14}$$

In (12)–(14) subscripts $_1$, $_2$, and $_3$ refer to quantities at angular frequencies ω_1, ω_2, and ω_3, respectively. The use of complex fields in (13) can largely simplify the following derivations.

In [3] it is assumed $\underline{\boldsymbol{h}}_3=0$ upon which $\underline{\boldsymbol{m}}_3$ was nonlinearly expressed in terms of $\underline{\boldsymbol{m}}_1,\underline{\boldsymbol{h}}_1,\underline{\boldsymbol{m}}_2$, and $\underline{\boldsymbol{h}}_2$. However, $\underline{\boldsymbol{h}}_3$ does not vanish, which together with $\underline{\boldsymbol{m}}_3$ must be determined from Maxwell equations. Actually, as we will point out later, the output intermodulation power will be proportional to $|h_{3\phi}|^2$, which would then lead to zero intermodulation coupling in Wu *et al.*'s calculations. In [3] Wu *et al.* related the intermodulation power at circulator ports by using the Faraday's law. They assumed e_{3z} to vanish at the ferrite disk center as the other two primary RF-electric components do, e_{1z} and e_{2z}. However, as revealed from (21), e_{3z} satisfies a different differential equation and hence there is no sufficient reason to make such an assumption. Also, Wu *et al.* calculated the output intermodulation power in terms of $|e_{3z}|^2$. However, discontinuity in e_{3z} can occur at the circulator-port junctions and evanescent modes will be present to make up this difference. Further discussion on this point will appear later in Section II.

For the $\exp(-i\omega_3 t)$ time dependence (13) gives the following magnetic constituent equation:

$$\underline{\boldsymbol{b}}_3=\underline{\boldsymbol{h}}_3+\underline{\boldsymbol{m}}_3=\underline{\underline{\boldsymbol{\mu}}}_3(\underline{\boldsymbol{h}}_3-\underline{\beta}) \tag{15}$$

$$\underline{\beta}=(\underline{\underline{\boldsymbol{I}}}-\underline{\underline{\boldsymbol{\mu}}}_3^{-1})\underline{\alpha} \tag{16}$$

and $\underline{\underline{\boldsymbol{\mu}}}_3$ is the regular Polder permeability tensor given by [6]–[8]

$$\underline{\underline{\boldsymbol{\mu}}}_3=\begin{pmatrix}\mu_3 & i\kappa_3 & 0\\ -i\kappa_3 & \mu_3 & 0\\ 0 & 0 & 1\end{pmatrix} \tag{17}$$

where μ_3 and κ_3 are

$$\mu_3=1+\frac{\omega_o\omega_m}{\omega_o^2-\omega_3^2},\quad \kappa_3=\frac{\omega_3\omega_m}{\omega_o^2-\omega_3^2} \tag{18}$$

and ω_m and ω_o are defined as

$$\omega_m=4\pi\gamma M_s$$
$$\omega_o=\gamma H_{\text{in}}.$$

Maxwell equations are

$$\nabla\times\underline{\boldsymbol{h}}_3=\frac{-i\epsilon\omega_3}{c}\underline{\boldsymbol{e}}_3,\quad \nabla\cdot\underline{\boldsymbol{b}}_3=0$$
$$\nabla\times\underline{\boldsymbol{e}}_3=\frac{i\omega_3}{c}\underline{\boldsymbol{b}}_3,\qquad \nabla\cdot\underline{\boldsymbol{e}}_3=0 \tag{19}$$

which, after assuming

$$h_{3z}=0=e_{3\rho}=e_{3\phi} \tag{20}$$

one derives

$$(\nabla^2+k_{3e}^2)e_{3z}=\frac{-i\omega_3\mu_{3e}}{c}(\nabla\times\underline{\beta})_z \tag{21}$$

$$h_{3\rho}=\frac{-ic}{\omega_3\mu_{3e}}\left[\frac{1}{\rho}\frac{\partial e_{3z}}{\partial\phi}+\frac{i\kappa_3}{\mu_3}\frac{\partial e_{3z}}{\partial\rho}\right]+\beta_\rho \tag{22}$$

$$h_{3\phi}=\frac{ic}{\omega_3\mu_{3e}}\left[\frac{-i\kappa_3}{\mu_3}\frac{1}{\rho}\frac{\partial e_{3z}}{\partial\phi}+\frac{\partial e_{3z}}{\partial\rho}\right]+\beta_\phi \tag{23}$$

where μ_{3e} is the Voigt permeability given by

$$\mu_{3e}=(\mu_3^2-\kappa_3^2)/\mu_3 \tag{24}$$

and the effective propagation constant k_{3e} is

$$k_{3e}=\omega_3(\mu_{3e}\epsilon)^{1/2}/c. \tag{25}$$

The complex dielectric constant ϵ in (19) and (22) is

$$\epsilon=\epsilon_f(1+i\tan\delta) \tag{26}$$

and ϵ_f and $\tan\delta$ are the dielectric constant and dielectric loss tangent of the ferrite material, respectively. In (22), (23), and (25) c denotes the speed of light in a vacuum.

We note that all of the above formulas derived for the induced cubic intermodulation fields at angular frequency ω_3

can be equally applied to the primary excitation fields at ω_1 and ω_2 provided that the driving terms described by $\underline{\alpha}$ or $\underline{\beta}$ are set to zero. That is, sources have been added to the forced oscillation at intermodulation frequency ω_3 such that the Helmholtz equation is now modified to include an inhomogeneous term to generate radiation at ω_3. Furthermore, the boundary conditions at the periphery of the ferrite disk must also be reinforced by the solution. From (21) the forced oscillation for cubic intermodulation results in an effective current distribution on the ferrite junction

$$\underline{j}_3 = \frac{c}{4\pi}(\nabla \times \underline{\beta})_z \tag{27}$$

which generates outgoing electromagnetic waves propagating toward the boundary of the ferrite disk. Meanwhile, the imposed magnetic-wall boundary conditions on the disk boundary not adjacent to the circulator ports are effective to reflect the incident electromagnetic waves such as to cancel the tangential components of the RF-magnetic fields there; only at the circulator ports the magnetic-wall boundary conditions are relaxed

$$\begin{aligned} h_{3\phi}(R,\phi) \neq \&0, \quad & \text{if } \phi_i - \theta_i \le \phi \le \phi_i + \theta_i, \\ & \text{for } 1 \le i \le 3N \\ = 0, \quad & \text{otherwise.} \end{aligned} \tag{28}$$

Here we have assumed the circulator to possess $3N$ ports which are located at $\phi = \phi_i$ with half-port suspension angle θ_i. The ferrite disk is of radius R. The three through-ports are numbered as 1, $1+N$, and $1+2N$, which are connected with matched loads and the other ports are connected with open-circuited stubs of finite length. For circulation action to occur we must assume three-fold symmetry on the circulator ports [7], [8].

Solutions to the intermodulation fields are therefore composed of two parts. The first-part solutions satisfy the homogeneous Helmholtz equation giving rise to the boundary conditions of (28), and the second-part solutions describe outgoing electromagnetic fields generated from the current distribution of (27). We refer to the first-part solutions by superscript $^{(0)}$ and the second-part solutions by superscript $^{(1)}$

$$\begin{aligned} e_{3z}(\underline{\rho}) &= e_{3z}^{(0)}(\underline{\rho}) + e_{3z}^{(1)}(\underline{\rho}) \\ h_{3\rho}(\underline{\rho}) &= h_{3\rho}^{(0)}(\underline{\rho}) + h_{3\rho}^{(1)}(\underline{\rho}) \\ h_{3\phi}(\underline{\rho}) &= h_{3\phi}^{(0)}(\underline{\rho}) + h_{3\phi}^{(1)}(\underline{\rho}). \end{aligned} \tag{29}$$

Green's function appropriate to the first-part solutions satisfies the homogeneous Helmholtz equation

$$(\nabla^2 + k_{3e}^2) G_{3z}^{(0)}(\rho,\phi;R,\phi') = 0 \tag{30}$$

whose boundary condition is that the tangential (ϕ-component) magnetic field vanishes at the disk periphery except for a delta-function excitation at $\rho = R$ and $\phi = \phi'$. From the Appendix we have

$$\begin{aligned} & G_{3z}^{(0)}(\rho,\phi;R,\phi') \\ & \quad = \frac{-iZ_{3f}}{2\pi} \sum_{n=-\infty}^{\infty} \frac{J_n(k_{3e}\rho) e^{in(\phi-\phi')}}{J_n'(k_{3e}R) + \dfrac{\kappa_3}{\mu_3}\dfrac{nJ_n(k_{3e}R)}{k_{3e}R}}. \end{aligned} \tag{31}$$

Here $J_n(x)$ and $J_n'(x)$ denote Bessel functions of the first kind of order n and its derivative, respectively. Z_{3f} is the wave impedance of the ferrite material at ω_3 and

$$Z_{3f} = \sqrt{\frac{\mu_{3e}}{\epsilon}}.$$

Green's function appropriate to the second-part solutions satisfies the inhomogeneous Helmholtz equation

$$\begin{aligned} & (\nabla^2 + k_{3e}^2) G_{3z}^{(1)}(\rho,\phi;\rho',\phi') \\ & \quad = -4\pi\delta(\rho-\rho')\delta(\phi-\phi')/\rho \end{aligned} \tag{32}$$

rendering the outgoing boundary condition at infinity. From [9] we have

$$\begin{aligned} & G_{3z}^{(1)}(\rho,\phi;\rho',\phi') \\ & \quad = i\pi H_0^{(1)}(k_{3e}\sqrt{\rho^2+\rho^2-2\rho\rho'\cos(\phi-\phi')}) \end{aligned} \tag{33}$$

where $H_0^{(1)}(x)$ is the Hankel function of the first kind of order zero. Note that $H_0^{(1)}(x)$ vanishes logarithmically as x goes to zero

$$H_0^{(1)}(x) \approx (2i/\pi)\,\ln(x), \quad \text{if } x \ll 1. \tag{34}$$

Therefore, solutions for the second part can be obtained as

$$\begin{aligned} e_{3z}^{(1)}(\rho,\phi) = {} & \frac{-\omega_3\mu_{3e}}{4c} \int_0^R \rho'\,d\rho' \int_0^{2\pi} d\phi' \\ & \cdot \left[\frac{\partial\beta_\phi(\underline{\rho}')}{\partial\rho'} - \frac{1}{\rho'}\frac{\partial\beta_\rho(\underline{\rho}')}{\partial\phi'}\right] \cdot \\ & \cdot H_0^{(1)}(k_{3e}\sqrt{\rho^2+\rho^2-2\rho\rho'\cos(\phi-\phi')}) \end{aligned} \tag{35}$$

$$\begin{aligned} h_{3\rho}^{(1)}(\rho,\phi) = {} & \left\{ \frac{i}{4} \int_0^R \rho'\,d\rho' \int_0^{2\pi} d\phi' \right. \\ & \cdot \left[\frac{\partial\beta_\phi(\underline{\rho}')}{\partial\rho'} - \frac{1}{\rho'}\frac{\partial\beta_\rho(\underline{\rho}')}{\partial\phi'}\right] \\ & \cdot \left[\frac{1}{\rho}\frac{\partial}{\partial\phi} + \frac{i\kappa_3}{\mu_3}\frac{\partial}{\partial\rho}\right] H_0^{(1)} \\ & \left. \cdot (k_{3e}\sqrt{\rho^2+\rho^2-2\rho\rho'\cos(\phi-\phi')}) \right\} \\ & + \beta_\rho(\underline{\rho}) \end{aligned} \tag{36}$$

$$\begin{aligned} h_{3\phi}^{(1)}(\rho,\phi) = {} & \left\{ \frac{-i}{4} \int_0^R \rho'\,d\rho' \int_0^{2\pi} d\phi' \right. \\ & \cdot \left[\frac{\partial\beta_\phi(\underline{\rho}')}{\partial\rho'} - \frac{1}{\rho'}\frac{\partial\beta_\rho(\underline{\rho}')}{\partial\phi'}\right] \\ & \cdot \left[\frac{-i\kappa_3}{\mu_3}\frac{1}{\rho}\frac{\partial}{\partial\phi} + \frac{\partial}{\partial\rho}\right] H_0^{(1)} \\ & \left. \cdot (k_{3e}\sqrt{\rho^2+\rho^2-2\rho\rho'\cos(\phi-\phi')}) \right\} \\ & + \beta_\phi(\underline{\rho}). \end{aligned} \tag{37}$$

In order to satisfy the boundary conditions of (28) for the overall intermodulation field the peripheral field-source needs

to be specified as the following:

$$S_3(\phi)=\begin{cases}0, & \text{if } \phi_i-\theta_i\le\phi\le\phi_i+\theta_i,\\ & \text{for } 1\le i\le 3N,\\ -h_{3\phi}^{(1)}(\phi), & \text{otherwise.}\end{cases} \tag{38}$$

This results in homogeneous-field excitation within the ferrite disk as

$$e_{3z}^{(0)}(\rho,\phi)=\frac{-iZ_f}{2\pi}\sum_{n=-\infty}^{\infty}\frac{A_nJ_n(k_{3e}\rho)e^{in\phi}}{J_n'(k_{3e}R)+\dfrac{\kappa_3}{\mu_3}\dfrac{nJ_n(k_{3e}R)}{k_{3e}R}} \tag{39}$$

$$h_{3\rho}^{(0)}(\rho,\phi)=\frac{-i}{2\pi}\sum_{n=-\infty}^{\infty}A_n\cdot\left[\frac{\dfrac{nJ_n(k_{3e}\rho)}{k_{3e}\rho}+\dfrac{\kappa_3}{\mu_3}J_n'(k_{3e}\rho)}{J_n'(k_{3e}R)+\dfrac{\kappa_3}{\mu_3}\dfrac{nJ_n(k_{3e}R)}{k_{3e}R}}\right]e^{in\phi} \tag{40}$$

$$h_{3\phi}^{(0)}(\rho,\phi)=\frac{1}{2\pi}\sum_{n=-\infty}^{\infty}A_n\cdot\left[\frac{J_n'(k_{3e}\rho)+\dfrac{\kappa_3}{\mu_3}\dfrac{nJ_n(k_{3e}\rho)}{k_{3e}\rho}}{J_n'(k_{3e}R)+\dfrac{\kappa_3}{\mu_3}\dfrac{nJ_n(k_{3e}R)}{k_{3e}R}}\right]e^{in\phi} \tag{41}$$

and the expansion coefficient A_n is given as

$$A_n=\int_0^{2\pi}d\phi'\,e^{-in\phi'}S_3(\phi'). \tag{42}$$

Therefore, provided that the first-order excitation fields $\underline{\boldsymbol{h}}_1$ and $\underline{\boldsymbol{h}}_2$ are known, the third-order coupled intermodulation field $\underline{\boldsymbol{h}}_3$ can now be completely calculated. The output intermodulation power at port j, $j=1$, $1+N$, and $1+2N$, can be estimated as

$$P_{3j}=|i_{3j}|^2Z_d/2 \tag{43}$$

where i_{3j} denotes the RF-current at ω_3 at port j, and Z_d is the wave impedance of the jth port

$$Z_d=\sqrt{\frac{1}{\epsilon_d}}.$$

Here ϵ_d denotes the dielectric constant of the dielectric-sleeve material surrounding the ferrite junction to match the circulator performance at circulation conditions [6]–[8]. Occasionally, the same piece of ferrite material is used both for the junction and for the matching sleeve, and only the junction area is locally biased by a vertical magnetic field. In this case $\epsilon_d=\epsilon_f$. The port current i_{3j} in (43) can be related to the transverse magnetic (TM) field surrounding the (stripline) port, h_{3j}, through Ampere's law

$$i_{3j}\approx 2\,w\,h_{3j}$$

and w denotes the width of the port. However, h_{3j} needs to be continuous across the junction boundary such that

$$h_{3j}=h_{3\phi}(R,\phi_j). \tag{44}$$

Here we have assumed that port j is a through port undermatched load and no RF-intermodulation field can be reflected back from port j. As such, the output intermodulation power at port j is derived as

$$P_{3j}=2\,w^2|h_{3\phi}(R,\phi_i)|^2Z_d. \tag{45}$$

A similar expression shall apply to the primary fields excited at ω_1 and ω_2. We note that in Wu *et al.*'s derivation [3] they assumed the output intermodulation power was related to $|e_{3z}(R,\phi_j)|^2$. However, the tangential electric field may experience discontinuity in passing across the junction boundary. For example, the tangential electric field drops to zero across a magnetic wall and the resultant discontinuity is compensated by fringing fields surrounding the wall boundary (that is, by inducing magnetic currents on the wall boundary).

In this paper we are only concerned with the calculations of the output intermodulation power as a function of the primary excitations applied at angular frequencies ω_1 and ω_2 (45). As such, we are only required to calculate $h_{3\phi}^{(1)}(R,\phi_j)$, since the homogeneous solution, (41), does not contribute to this RF-field as specified by the boundary condition (38)

$$h_{3\phi}^{(0)}(R,\phi_j)=0.$$

Therefore, the only task to perform is the evaluation of the double integral appearing in (37) for the calculation of $h_{3\phi}^{(1)}(R,\phi_j)$. This can be accomplished by applying an equally-spaced grid over a 2D rectangular area defined by $0\le\phi\le 2\pi, 0\le\rho\le R$; differentiation and integration can then be performed by using finite difference methods. However, in order to avoid self-field singularity associated with Hankel function at the origin (34), a closed-type integration scheme which includes direct evaluation of the integrand at $\rho=R$, should not be used. Instead, we have used Newton–Cotes formulas of open type in calculating $h_{3\phi}^{(1)}(R,\phi_j)$ in (37). The grid points employed were 40 × 40, and the convergence is quite good (more than five significant digits).

To complete the formulation of the paper, we summarize in the following the expressions for the primary fields excited at ω_1 and ω_2 [6]–[8]. Similar notations will be used as before and subscript $_3$ will be dropped hereafter. The interport impedance for a $3N$-port circulator is

$$G_{ij}=-iZ_f\left(\frac{\theta_j}{\pi}\right)\sum_{n=-\infty}^{\infty}\left[\frac{n}{x}\left(1+\frac{\kappa}{\mu}\right)-\frac{J_{n+1}(x)}{J_n(x)}\right]^{-1}\cdot\left(\frac{\sin\,n\theta_i}{n\theta_i}\right)\left(\frac{\sin\,n\theta_j}{n\theta_j}\right)e^{in(\phi_i-\phi_j)} \tag{46}$$

where x is defined as

$$x=k_{\text{eff}}R$$

and k_{eff} can be obtained by a similar expression of (25). Let the primary field be excited at port 1 with an incident amplitude in h_ϕ as $(h_\phi)_{\text{in}}$. We denote the amplitude of h_ϕ in port j as

a_j, $1 \le j \le 3N$. We have then

$$\sum_{j=1}^{3N}(Z_i\delta_{ij}+G_{ij})a_j = 2Z_d(h_\phi)_{\mathbf{in}}\delta_{i1} \tag{47}$$

where Z_j denote the wave impedance of port j and

$$Z_j = \begin{cases} Z_d, & \text{if } j = 1, 1+N, 1+2N, \\ iZ_d\ \cot(x_j\omega\sqrt{\epsilon_d})/c, & \text{otherwise.} \end{cases} \tag{48}$$

Here x_j is the length of the open-circuited port j. After a_j's have been solved from (47), the modal expansion coefficient c_j expressed in (A4)–(A6) of the Appendix can then be derived as

$$c_n = \frac{-i}{\pi}Z_f\left[J_n'(x)+\frac{\kappa}{\mu}\frac{nJ_n(x)}{x}\right]^{-1} \cdot\sum_{j=1}^{3N}\left[\frac{a_j\ \sin\ n\theta_j}{n}\exp(-in\phi_j)\right]. \tag{49}$$

Therefore, $\underline{\boldsymbol{h}}_1$ and $\underline{\boldsymbol{h}}_2$ can be obtained. The magnetization fields are then

$$\underline{\boldsymbol{m}} = (\underline{\underline{\boldsymbol{\mu}}} - \underline{\underline{\boldsymbol{I}}})\underline{\boldsymbol{h}} \tag{50}$$

which, together with $\underline{\boldsymbol{h}}_1$ and $\underline{\boldsymbol{h}}_2$, are used in (14) and (16) to obtain the cubic intermodulation excitation terms (35)–(37). The input signal power at ω_1 and ω_2 can be calculated from (45) with $h_{3\phi}(R,\phi_i)$ being replaced by $(h_\phi)_{\mathbf{in}}$.

III. Results

We consider the three-port very high frequency (VHF) circulator design reported in [3]. In [3] the circulator was given the following parameters: $4\pi M_s = 600$ G, $H_o = 800$ Oe, $\epsilon_f = 16$. We assume the same ferrite was used as the matching sleeve material such that $\epsilon_d = \epsilon_f = 16$. In order to approximately give the center transmission frequency around 140 MHz, we further assume $R = 8$ cm. Also, we have assumed $\Delta H = 60$ Oe at $f_r = 10$ GHz, and $\tan\delta = 0.0001$. Circulation condition [8] can then be solved which requires a half-port suspension angle $\theta = 0.112$ rd, and the center transmission frequency f_c occurs at 0.1414 GHz. The calculated scattering parameters of the circulator are shown in Fig. 1. The insertion loss at f_c was calculated to be -0.139 dB due to the imposed material losses. We note that the circulator exhibits narrow-band transmission, since it is a three-port circulator biased above ferrimagnetic resonance. A high-power circulator needs to be biased above resonance in order to remove magnetic domain walls. Wide-band circulator biased above FMR resonance can be obtained by using a six-port design [7]–[8].

In the following calculations we consider the two primary signals to be applied at port 1 and the generated cubic intermodulation signals are measured at the transmission port 2. Port 3 is the isolation port, which is terminated by a matched load. Fig. 2 shows the calculated intermodulation

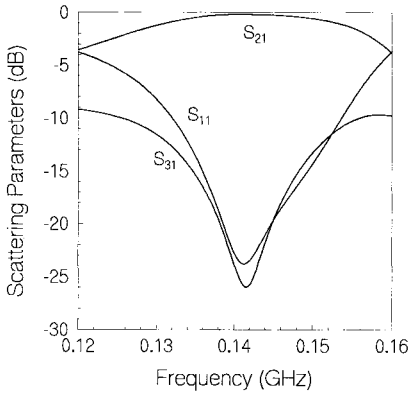

Fig. 1. Calculated scattering parameters of the VHF circulator reported in [1].

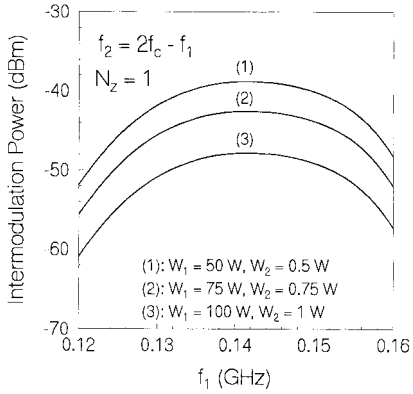

Fig. 2. Calculated intermodulation power output for $f_2 = 2f_c - f_1$ and $N_z = 1$.

output power as a function of f_1 using $f_2 = 2f_c - f_1$. The axial demagnetizing factor considered is $N_z = 1$. Three power levels have been considered, $W_1 = 50$ W and $W_2 = 0.5$ W, $W_1 = 75$ W and $W_2 = 0.75$ W, and $W_1 = 100$ W and $W_2 = 1$ W. From Fig. 2 it is seen that maximum intermodulation occurs when f_1 and f_2 are located close to the center frequency f_c, which exhibits the following values: -47.8 dBm for $W_1 = 50$ W and $W_2 = 0.5$ W, -42.6 dBm for $W_1 = 75$ W and $W_2 = 0.75$ W, and -38.9 dBm for $W_1 = 100$ W and $W_2 = 1$ W. These numbers compare very well with measurements [3]: -44 dBm when $W_1 = 50$ W and $W_2 = 0.5$ W, and -42 dBm when $W_1 = 75$ W and $W_2 = 0.75$ W. However, exact comparison between theory and experiments is not possible, since the exact parameters of the circulator are not known (the center transmission frequency used in this calculational model is 144.4 MHz, whereas the center transmission frequency measured in [3] was 124 MHz). We note that in Fig. 2 intermodulation levels drop off when f_1, and hence f_2, deviate from f_c. This is due to the fact that the amplitudes of the primary fields, $\underline{\boldsymbol{h}}_1, \underline{\boldsymbol{m}}_1, \underline{\boldsymbol{h}}_2$, and $\underline{\boldsymbol{m}}_2$, decrease as a consequence of the frequency shift away from circulation conditions.

Fig. 3 shows the calculated intermodulation output power as a function of f_1 using $f_2 = f_c$. Again, we have assumed $N_z = 1$ and have used the same three power levels: $W_1 = 50$ W and $W_2 = 0.5$ W, $W_1 = 75$ W and $W_2 = 0.75$ W, and

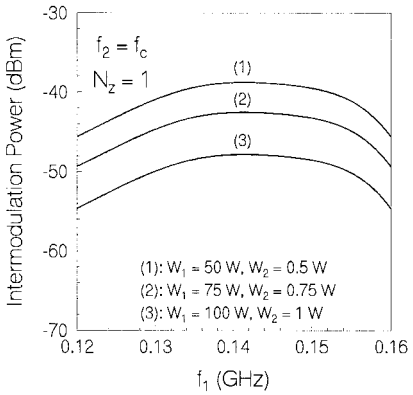

Fig. 3. Calculated intermodulation power output for $f_2 = f_c$ and $N_z = 1$.

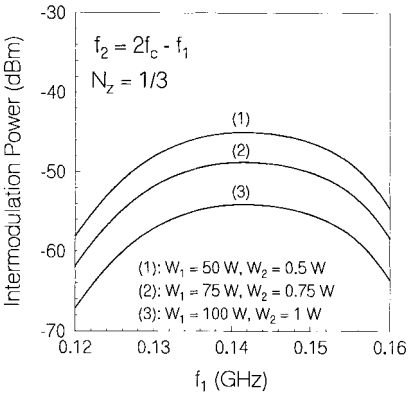

Fig. 4. Calculated intermodulation power output for $f_2 = 2f_c - f_1$ and $N_z = 1/3$.

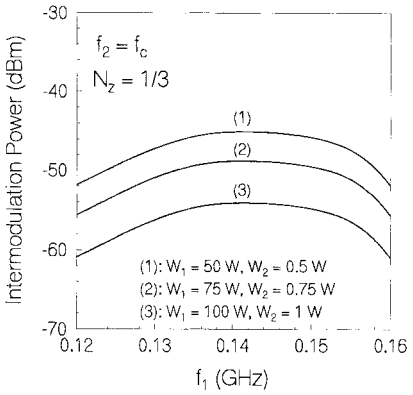

Fig. 5. Calculated intermodulation power output for $f_2 = f_c$ and $N_z = 1/3$.

$W_1 = 100$ W and $W_2 = 1$ W. Maximum intermodulation occurs at the same frequencies and levels as in Fig. 2, since the power maxima are identically the same for these two cases: $f_1 = f_2 = f_c$. However, intermodulation power levels off more rapidly in the former case when $f_2 = 2f_c - f_1$, since for this case $\underline{\boldsymbol{h}}_2$ and $\underline{\boldsymbol{m}}_2$ presume smaller values than the latter case when $f_2 = f_c$.

Figs. 4 and 5, respectively, show the same results as Figs. 2 and 3 except that the axial demagnetizing factor N_z has been lowered to a smaller value: $N_z = 1/3$. For these calculations maximum intermodulation still occurs at the center transmission frequency which exhibits the following values: -54.2 dBm for $W_1 = 50$ W and $W_2 = 0.5$ W, -49.8 dBm for $W_1 = 75$ W and $W_2 = 0.75$ W, and -45.2 dBm for $W_1 = 100$ W and $W_2 = 1$ W. These values are about 5–6 dBm smaller than those previous values calculated for $N_z = 1$. Therefore, we conclude that the static demagnetization of the ferrite disk has an adverse effect in generating cubic intermodulation for channel coupling. A quiet circulator can be obtained if the demagnetizing field is minimized. In the past, Schloemann and Blight have applied two polycrystalline YIG domes in the shape of semispheres covering the ferrite circuit from above and below to produce a uniform internal bias field within the ferrite disk [10]. As such, $N_z = 1/3$, and ultra-wide bandwidth was obtained for circulator transmission [10]. For nonlinear applications, we conclude that the static demagnetization is responsible for spin-wave instabilities near subsidiary absorption during ferrimagnetic resonance [4], reduction of echo-gain amplification for ferrimagnetic echoing in the time-domain [1], [2], and generation of higher intermodulation coupling among channels in the frequency domain. The demagnetizing fields should therefore be avoided in all of these applications.

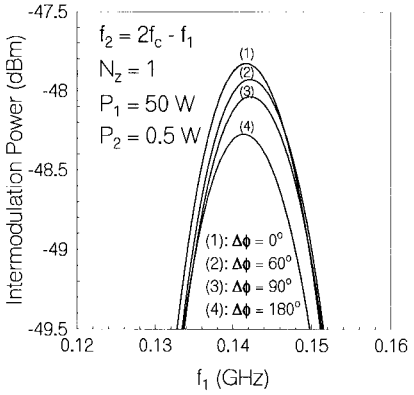

Fig. 6. Calculated intermodulation power output considering interference between input signals: $f_2 = 2f_c - f_1$.

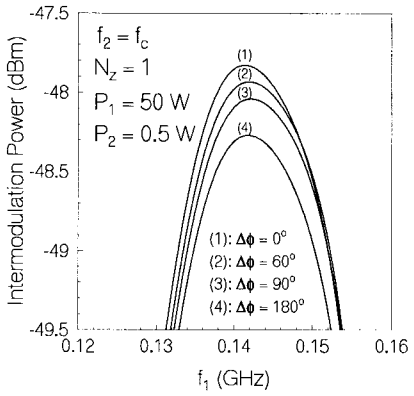

Fig. 7. Calculated intermodulation power output considering interference between input signals: $f_2 = f_c$.

In the above calculations we have assumed the two primary fields are applied at the same phases. If the input phases are not equal, intermodulation level will differ accordingly. This is shown in Figs. 6 and 7 where the intermodulation power is plotted as a function of f_1 using $f_2 = 2f_c - f_1$ and $f_2 = f_c$,

respectively. The input powers are $W_1 = 50$ W and $W_2 = 0.5$ W, and the axial demagnetizing factor considered is $N_z = 1$. From Figs. 6 and 7 it is seen that the generated intermodulation power decreases for increasing phase difference between the two input signals. From in-phase coupling $\Delta\phi = 0°$ to out-of-phase coupling $\Delta\phi = 180°$ the output intermodulation power has been decreased in an amount equal to 0.55 dBm, indicating the interference nature of the cubic intermodulation interaction. The difference between Figs. 6 and 7 can be understood from the same basis applied to Figs. 2 and 3.

IV. Conclusion

We have formulated the nonlinear intermodulation problem for a ferrite junction circulator. The equation of motion of the magnetization vector has been approximated up to the third order in the RF-excited fields and the coupled Maxwell equations have been solved analytically. We found that the cubic intermodulation exhibits maximum coupling when the signal channels are close to the center transmission frequency of the circulator. The static demagnetization factor of the ferrite shows adverse effects in increasing the intermodulation levels, and hence it should be minimized for a quiet circulator design. Finally, the calculated intermodulation power shows interference coupling when the primary signals are applied at different phases.

Appendix

From Maxwell equations the RF-electromagnetic field in a source-free 2D ferrite junction satisfy the following differential equations [5]–[7]

$$(\nabla^2 + k_{\text{eff}}^2)e_z = 0 \tag{A1}$$

$$h_\rho = \frac{-ic}{\omega\mu_{\text{eff}}}\left[\frac{1}{\rho}\frac{\partial e_z}{\partial\phi} + \frac{i\kappa}{\mu}\frac{\partial e_z}{\partial\rho}\right] \tag{A2}$$

$$h_\phi = \frac{ic}{\omega\mu_{\text{eff}}}\left[\frac{-i\kappa}{\mu}\frac{1}{\rho}\frac{\partial e_z}{\partial\phi} + \frac{\partial e_z}{\partial\rho}\right] \tag{A3}$$

where k_{eff} and μ_{eff} are effective propagation constant and effective permeability of the ferrite material given by similar expressions of (18), (24), and (25). Solutions to the above equations regular at the disk center can be written as

$$e_z(r,\phi) = \sum_{n=-\infty}^{\infty} c_n J_n(kr)e^{in\phi} \tag{A4}$$

$$h_\phi(r,\phi) = \frac{1}{Z_f}\sum_{n=-\infty}^{\infty} c_n\left[J_n'(kr) + \frac{\kappa}{\mu}\frac{nJ_n(kr)}{kr}\right]e^{in\phi} \tag{A5}$$

$$h_\rho(r,\phi) = \frac{i}{Z_f}\sum_{n=-\infty}^{\infty} c_n\left[\frac{nJ_n(kr)}{kr} + \frac{\kappa}{\mu}J_n'(kr)\right]e^{in\phi} \tag{A6}$$

and Z_f is similar to Z_{3f} defined as before. Let us now assume the boundary condition for h_ϕ to be

$$h_\phi(R,\phi) = \delta(\phi - \phi_i). \tag{A7}$$

This solves c_n from (A6) as

$$c_n = \frac{-iZ_f}{2\pi}\left[J_n'(k_{\text{eff}}R) + \frac{\kappa}{\mu}\frac{nJ_n(k_{\text{eff}}R)}{(k_{\text{eff}}R)}\right]^{-1} \tag{A8}$$

and hence the RF-electric field is

$$e_z^{(0)}(\rho,\phi) = \frac{-iZ_f}{2\pi}\sum_{n=-\infty}^{\infty}\frac{J_n(k_{\text{eff}}\rho)e^{in(\phi-\phi')}}{J_n'(k_{\text{eff}}R) + \frac{\kappa}{\mu}\frac{nJ_n(k_{\text{eff}}R)}{k_{\text{eff}}R}} \tag{A9}$$

which is used in the text as the Green's function $G_{3z}^{(0)}(\rho,\phi;R,\phi')$.

References

[1] H. How and C. Vittoria, "Theory on amplified ferrimagnetic echoes," *Phys. Rev. Lett.*, vol. 66, p. 1626–1629, 1991.

[2] ———, "Amplification factor of echo signals in ferrimagnetic materials," IEEE *Trans. Microwave Theory Tech.*, vol. 39, p. 1828–1835, 1991.

[3] Y.-S. Wu, W. H. Ku, and J. E. Erickson, "A study of nonlinearities and intermodulation characteristics of 3-port distributed circulators," *IEEE Trans. Microwave Theory Tech.*, vol. MTT-24, p. 69–77, 1976.

[4] H. Suhl, "The theory of ferromagnetic resonance at high signal powers," *J. Phys. Chem. Solids*, vol. 1, p. 209–227, 1957.

[5] H. How, R. C. O'Handley, and F. R. Morgenthaler, "Soliton theory for realistic domain wall dynamics," *Phys. Rev. B*, vol. 40, p. 4809–4817, 1989.

[6] H. How, C. Vittoria, and C. Carosella, "Novel filter design incorporating stripline Y-junction circulators," *IEEE Trans. Microwave Theory Tech.*, vol. 39, p. 40–46, 1991.

[7] H. How, R. Schmidt, and C. Vittoria, "Design of six-port ferrite junction circulators: theory and experiments," *IEEE Trans. Microwave Theory Tech.*, vol. 42, p. 1272–1275, 1994.

[8] H. How, T.-M. Fang, C. Vittoria, "Losses in multiport stripline/microstrip circulators," to be published.

[9] P. M. Morse and H. Feshbach, *Methods of Theoretical Physics*. New York: McGraw-Hill, 1953.

[10] E. Schloemann and R. E. Blight, "Broad-band stripline circulators based YIG and Li-ferrite single crystals," *IEEE Trans. Microwave Theory Tech.*, vol. MTT-34, p. 1394–1400, 1986.

Hoton How, photograph and biography not available at the time of publication.

Carmine Vittoria (F'90), photograph and biography not available at the time of publication.

Ronald Schmidt (F'84), photograph and biography not available at the time of publication.